CCD BVI PHOTOMETRY OF THE SOUTHERN OPEN CLUSTERS PISMIS 23 AND BH 222

JUAN J. CLARIÁ[1] and ANDRÉS E. PIATTI[2]

[1]*Observatorio Astronómico, Córdoba, Argentina*
[2]*Instituto de Astronomía y Física del Espacio, Buenos Aires, Argentina;*
E-mail: claria@oac.uncor.edu

Abstract. *CCD BVI* Johnson–Cousins photometry of the open cluster candidates Pismis 23 and BH 222 is presented. Both the analysis of the colour-magnitude diagrams and star counts performed in the regions of these two objects support their physical reality. For Pismis 23 we derive $E(B-V) = 2.0 \pm 0.1$, $E(V-I) = 2.6 \pm 0.1$, a distance from the Sun $d = (2.6 \pm 0.6)$ kpc and an age of (300 ± 100) Myr, while for BH 222 we obtain $E(V-I) = 2.\,4 \pm 0.2$, $d = (6.0 \pm 2.7)$ kpc and (60 ± 30) Myr. Both objects, located beyond the Sagittarius arm, are among the most reddened and distant open clusters known in the direction towards the Galactic centre.

Keywords: open clusters-Pismis 23, BH 222-photometry

1. Observations

Pismis 23, also known as Lyngå 10 (Lyngå, 1965), BH 190 (van den Bergh and Hagen, 1975) or ESO226-SC5 (Lauberts, 1982), was first identified as an open cluster by Pismis (1959), while BH 222 was first detected by van den Bergh and Hagen (1975). None of these two stellar groups have been studied previously. We obtained *CCD BVI* Johnson–Cousins images in the fields of Pismis 23 and BH 222 with a 0.6-m telescope at the Las Campanas Observatory, Chile. The observations were performed with a PM 512 × 512 chip, covering a field of 4×4 arcmin^2. The IRAF/DAOPHOT package was used to reduce the observations in the standard way at the Observatorio Astronómico de Córdoba (Argentina). (V magnitudes and $(B-V)$ and $(V-I)$ colours in the two cluster fields are available upon request to the first author.)

2. Colour-Magnitude Diagrams

Figure 1 shows the $(V, B-V)$ and $(V, V-I)$ diagrams of stars in the fields of Pismis 23 (top) and BH 222 (bottom). They reveal a difference of ∼1.0–1.5 mag in the limiting magnitudes reached between both diagrams, this effect being mainly caused by a strong interstellar extinction. The fiducial cluster sequences such as the cluster Main Sequences (MSs) and, if any, the giant and/or supergiant

Astrophysics and Space Science **290:** 353–362, 2004.

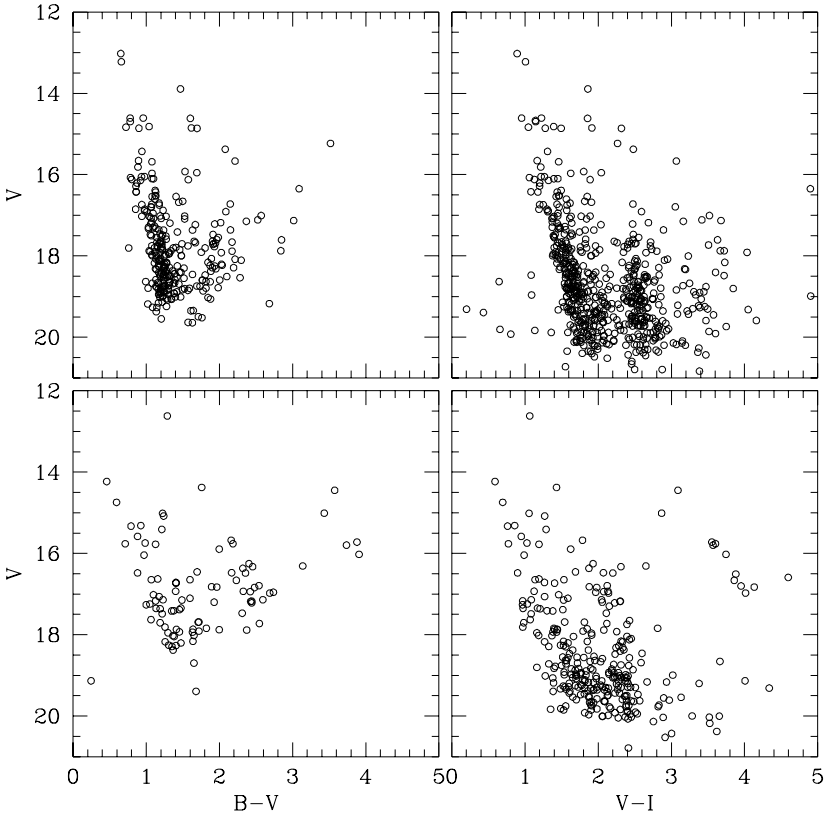

Figure 1. $(V, B-V)$ and $(V, V-I)$ colour-magnitude diagrams of stars in the field of Pismis 23 (top) and BH 222 (bottom).

star sequences are not easily recognizable. The long and blue tilted star sequence corresponds in the colour-magnitude diagrams (CMDs) of Pismis 23 to field MS stars belonging to the young disk (age $\sim$ 4.5 Gyr, $Z \approx 0.018$–0.022), to the intermediate-age disk (age $\sim$ 4.5–7.0 Gyr, $Z \approx 0.008$–0.015), and, at its fainter portion, to the old disk population (age $\sim$ 7.0–10.0 Gyr, $Z \approx 0.003$–0.008), according to the statistical results obtained by Ng et al. (1996). The cluster MS should be represented by the numerous stars that define the broad and disperse sequence of redder colours, clearly seen in the $(V, V-I)$ diagram at $V-I \sim 2.4$–2.8.

The tilted blue sequence in the CMDs of BH 222, comparable to the one in the CMDs of Pismis 23 but clearly less populous, is also composed by field MS stars. A comparison between the $(V, V-I)$ CMDs of both clusters lead to the conclusion that the redder sequence in BH 222 corresponds to the cluster MS.

3. Pismis 23

We traced a circle of 13.5 arcsec to encompass the innermost cluster region and an ellipse with minor (b) and major (a) semi-axes of 27 and 36 arcsec respectively, the direction of the latter being defined by a position angle of 75° (Figure 2). The resulting CMDs shown in Figure 3 demonstrate that most of the stars distributed inside the extracted areas fall along the red sequence. Note that an excess of stars confined to a small region in the sky can develop a sequence with a different lower envelope from that of a field star sequence only if they have a common origin. This fact strongly confirms that Pismis 23 is a real cluster.

We identified as many stars as possible in a red DSS image of 15 arcmin on a side centred on the object and counted field stars within 100 circles selected randomly and spread throughout the DSS image, discarding those circular regions superimposed on a circle of the same dimension centred on the object. The averaged

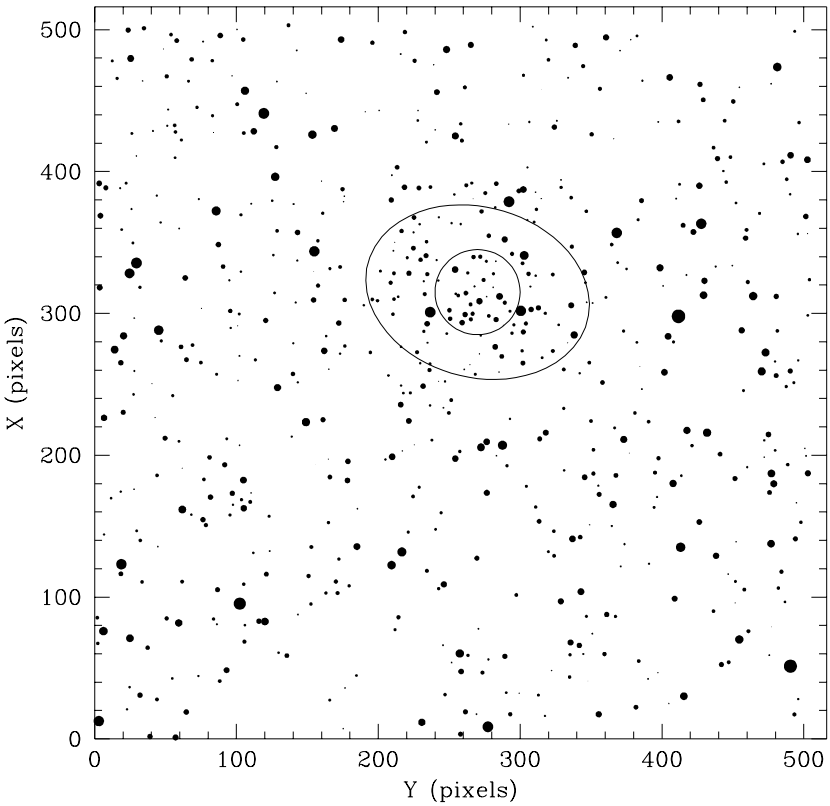

Figure 2. Schematic finding chart for the field of Pismis 23. Two circular and elliptical extractions are also shown. North is up and East is to the left. The sizes of the plotting symbols are proportional to the *V* magnitude of the stars.

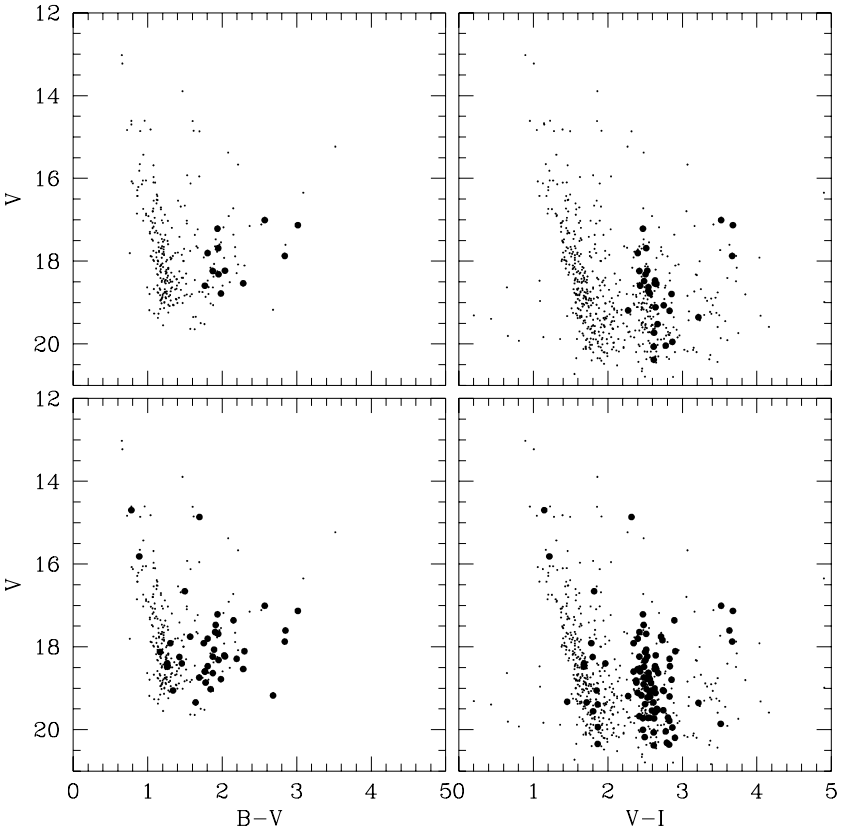

Figure 3. $(V, B-V)$ and $(V, V-I)$ colour-magnitude diagrams of stars in the field of Pismis 23: all measured stars (dots), circular extraction (filled circles, top) and elliptical extraction (filled circles, bottom).

star density in the field turned out to be 24 ± 4 stars/arcmin^2, while we counted 53 stars/arcmin^2 in the cluster circle having the same area as each field. This value doubles the mean field star density and is in full agreement with the cluster reality of Pismis 23.

We estimated the fundamental cluster parameters by fitting isochrones to the observed $(V, V-I)$ CMD, using different sets of isochrones computed by the Geneva (Lejeune and Schaerer, 2001, hereafter LS01) and Padova (Girardi et al., 2000, hereafter GBBC00) groups. We adopted a solar metal content ($Z = 0.02$) for the cluster, although we would have obtained similar cluster parameters if we had used adjacent metallicity values from the model grids ($Z = 0.008$ or 0.04). We adjusted the cluster MS using the position of the cluster red giants as reference. The isochrone that best fitted the cluster sequences turned out to be that of $\log t = 8.5$ of GBBC00, equivalent to $\sim$300 Myr, as shown in Figure 4. Figure 5 shows that the isochrone for $\log t = 8.5$ calculated from the stellar evolutionary models of LS01 compares very well with that of GBBC00. Nonetheless, since the loop at

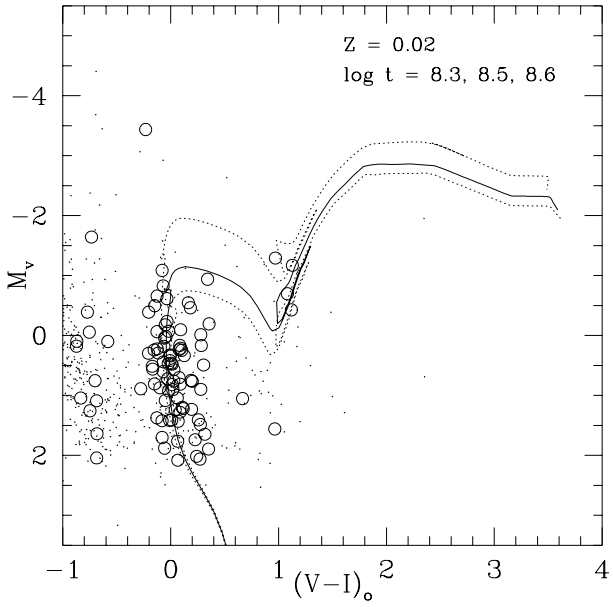

Figure 4. M_V vs. $(V-I)_0$ colour-magnitude diagram for Pismis 23 with the theoretical isochrones for $\log t = 8.3$, 8.5 and 8.6 of Girardi et al. (2000) superimposed. Stars distributed within the elliptical extraction are represented by open circles.

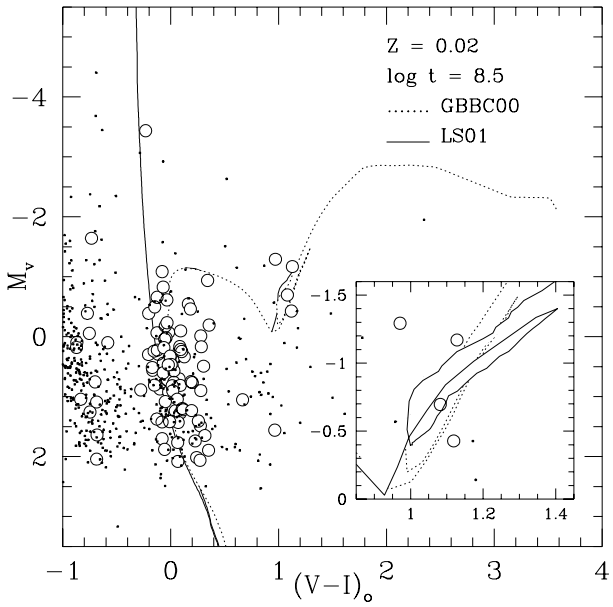

Figure 5. M_V vs. $(V-I)_0$ colour-magnitude diagram for Pismis 23 with the ZAMS and the theoretical isochrones for $\log t = 8.5$ computed by Girardi et al. (2000, GBBC00, dotted line) and Lejeune and Schaerer (2001, LS01, solid line) superimposed. An enlargement of the giant clump region is shown at the lower-right corner. Symbols are the same as in Figure 4.

the He burning stage in the GBBC00's isochrone results slightly steeper, a more suitable fit is obtained for the giant stars from this isochrone.

To estimate the $E(B-V)$ colour excess for the cluster, we used the resulting apparent distance modulus ($V-M_V = 18.30 \pm 0.25$) and the Zero-Age Main Sequence (ZAMS) of Schmidt–Kaler (1982). Using this value and the $E(V-I)$ colour excess obtained from the isochrone fit, we derived a colour-to-colour $E(V-I)/E(B-V)$ ratio of 1.3 ± 0.5, which indicates that the absorption in the direction towards the cluster follows approximately the normal extinction law. We then adopted the most frequently used values of 1.33 and 3.2 for the $E(V-I)/E(B-V)$ and $A_V/E(B-V)$ ratios (Cousins, 1978) to estimate the cluster distance.

4. BH 222

We employed a similar strategy to analyse the CMDs of BH 222. We carried out circular and elliptical extractions of the most populated regions on the deepest I

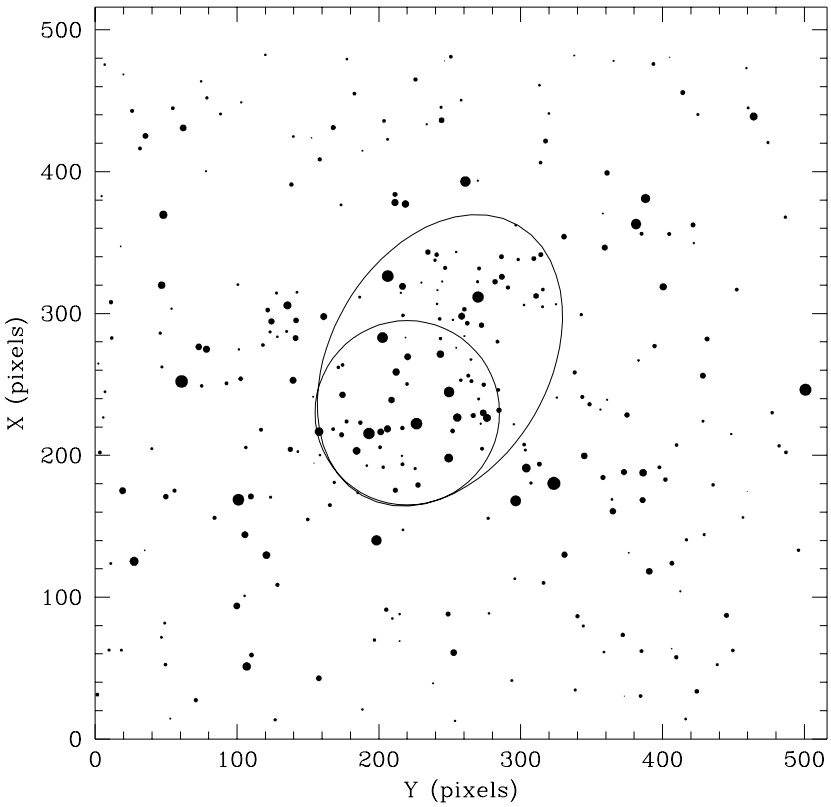

Figure 6. Schematic finding chart for the field of BH 222. Two circular and elliptical extractions are also shown. North is up and East is to the left. The sizes of the plotting symbols are proportional to the I magnitude of the stars.

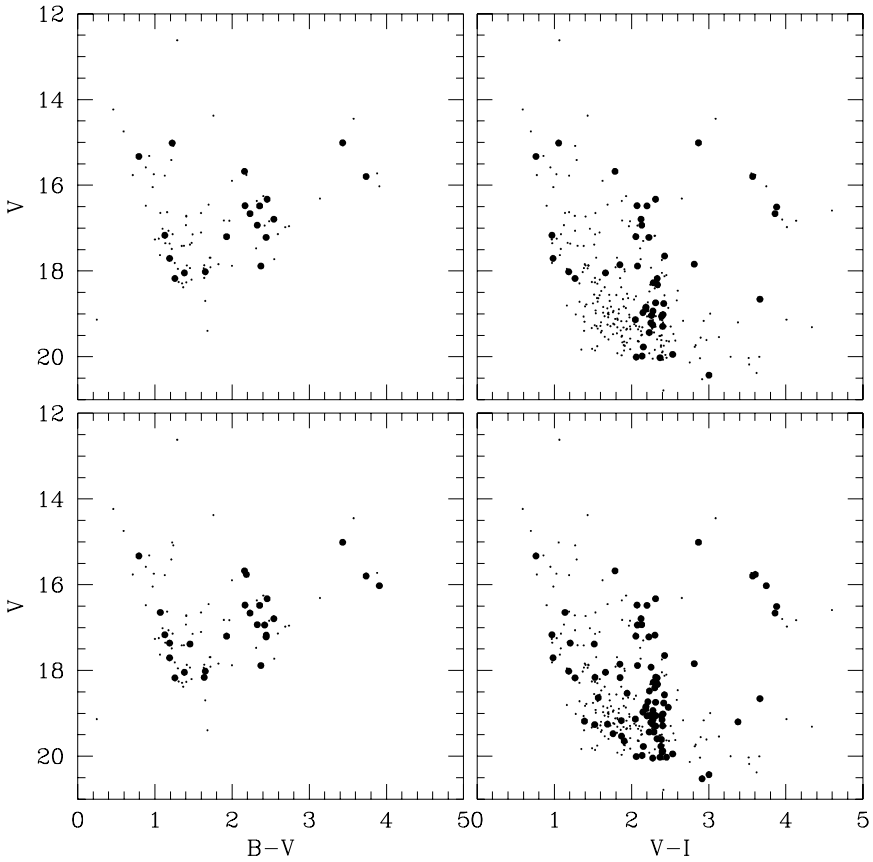

Figure 7. $(V, B-V)$ and $(V, V-I)$ colour-magnitude diagrams of stars in the field of BH 222: all measured stars (dots), circular extraction (filled circles, top) and elliptical extraction (filled circles, bottom).

frame and built the corresponding CMDs. Figure 6 shows the obtained schematic finding chart for all the stars with at least one measurement in the I passband. The positions and dimensions of the circle and the ellipse drawn in Figure 6 were chosen as an attempt to delineate the nuclear parts of the cluster and its boundary. Figure 7 reproduces the $(V, B-V)$ and $(V, V-I)$ CMDs of the stars observed in the field of BH 222 and shows the loci of the stars (filled circles) distributed within the circular (top panels) and elliptical (bottom panels) extractions, respectively. The distribution of the extracted stars in the $(V, V-I)$ diagram closely resembles that of a vertical MS with very red luminous stars, typically red supergiants, of a younger cluster. The cluster MS presents a small colour offset at $V \sim 18$ mag, which causes the brighter stars to appear slightly bluer. Stars belonging to both parts of this 'cracked' MS are mostly supposed to be cluster stars, a fact from which we believe that this apparent break is caused by a non-uniform interstellar absorption across the cluster field.

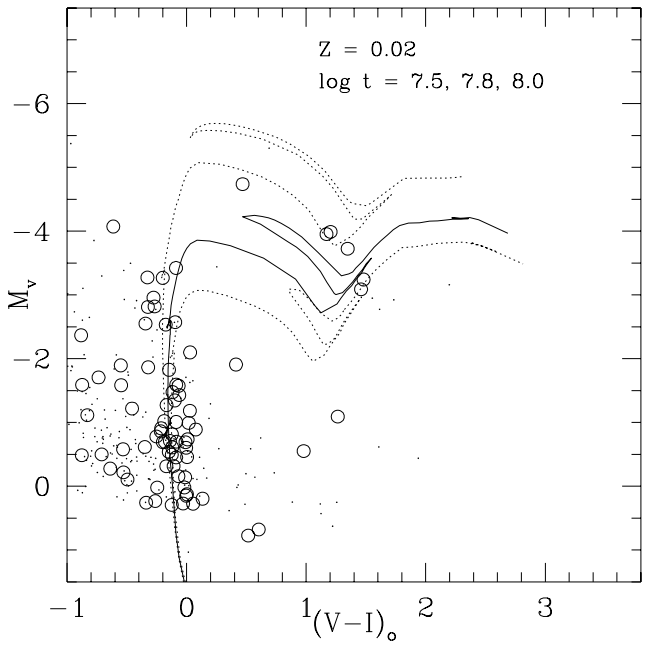

Figure 8. M_V vs. $(V-I)_0$ colour-magnitude diagram for BH 222 with the theoretical isochrones for $\log t = 7.5$, 7.8 and 8.0 of Salasnich et al. (2000) superimposed. Stars distributed within the elliptical extraction are represented by open circles.

We also performed star counts in the field of BH 222 following the same precepts as for Pismis 23 and found a mean density of 17 ± 3 stars/arcmin^2, while we counted 40 stars/arcmin^2 in the surrounding field. These values corroborate the physical existence of BH 222.

From isochrone fittings we determined $E(V-I) = 2.4 \pm 0.2$, $V - M_V = 19.7 \pm 0.5$, and an age of (60 ± 30) Myr (Figure 8). As for the Padova group, we used the isochrones computed by Salasnich et al. (2000), since they extended those of GBBC00 towards younger ages. Although there exists a tight agreement between the positions of the red supergiant stars (RSGs) and the theoretical red giant branch (Figure 9), the latter results $\sim$0.6 mag bluer than the RSGs. For this reason, we considered the cluster MS and the bottom of the He burning phase to estimate the mean cluster reddening and apparent distance modulus, respectively. The $V - I$ colour difference between RGSs and the isochrones probably arises not only from the effect of differential reddening, but also from the input physics and evolutionary codes used. In Figure 9 the isochrones have been shifted to obtain the best fit with the observed points. This figure shows how the RGS phase in the isochrone of LS01 turns out to be redder than the corresponding loop in the isochrone of Salasnich et al. (2000). Likewise, we did not find a noticeable difference in the fit if isochrones with high mass loss for massive stars were used.

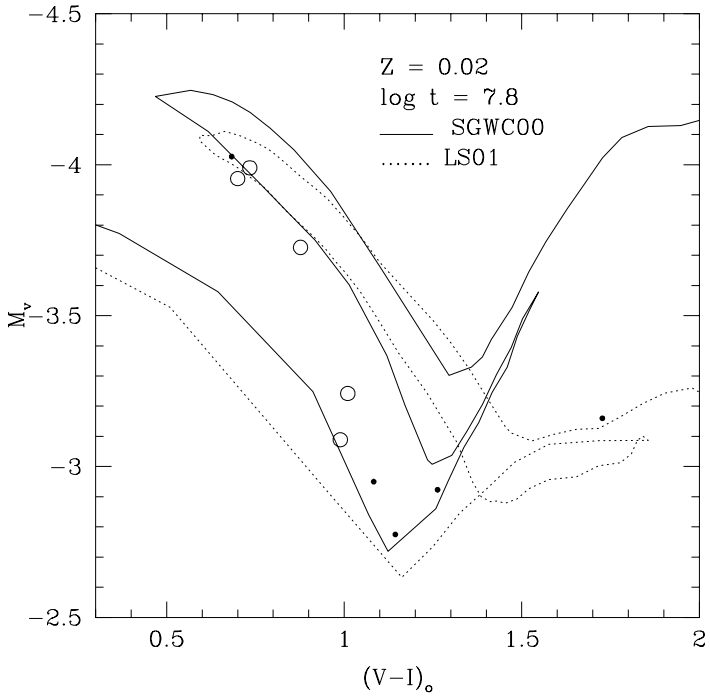

Figure 9. Giant clump region of the M_V vs. $(V-I)_0$ colour-magnitude diagram for BH 222 with the theoretical isochrones for $\log t = 7.8$ computed by Salasnich et al. (2000, SGWC00, solid line) and Lejeune and Schaerer (2001, LS01, dotted line) superimposed. The isochrones were shifted to obtain the best match with giant clump stars. Symbols are the same as in Figure 8.

5. Discussion

The resulting parameters place these two objects among the most reddened and distant open clusters located in the direction towards the Galactic centre. Using the WEBDA database, we selected a list of clusters distributed within a solid angle centred at the midst of both clusters, defined by $332^\circ \leq l \leq 352^\circ$ and $-2.5^\circ \leq b \leq 2.5^\circ$, and with known values of their colour excess and distances. We find that only three clusters (Ruprecht 119, NGC 6216 and Havlen-Moffat 1) are more distant than Pismis 23. The distances estimated for Pismis 23 and BH 222 placed them beyond the Sagittarius arm, close to the direction where this arm probably bifurcates into two arms (Vogt and Moffat, 1975). With the sole exception of Westerlund 1 ($E(B-V) = 4.3$; Piatti et al. 1998), Pismis 23 and BH 222 are among the clusters affected by the highest $E(B-V)$ colour excesses.

References

Cousins, A.W.J.: 1978, *MNRAS* **37**, 62.
Girardi, L., Bressan, A., Bertelli, G. and Chiosi, C.: 2000, *A&AS* **141**, 371 (GBBC00).

Lauberts, A.: 1982, *The ESO/Uppsala Survey of the ESO(B) Atlas*, ESO, Garching, Germany.
Lejeune, T. and Schaerer, D.: 2001, *A&A* **366**, 538 (LS01).
Lyngå, G.: 1965, Medd. fran Lunds Observatorium, Ser. II, No. 143.
Ng, Y.K., Bertelli, G., Chiosi, C. and Bressan, A.: 1996, *A&A* **310**, 771.
Piatti, A.E., Bica, E. and Clariá, J.J.: 1998, *A&AS* **127**, 423.
Pismis, P.: 1959, *Bol. Tonantzintla y Tacubaya* **18**, 37.
Salasnich, B., Girardi, L., Weiss, A. and Chiosi, C.: 2000, *A&A* **361**, 1023.
Schmidt-Kaler, Th.: 1982, in: K. Schaifers and H.H. Voigt (eds.), *Landolt-Bornstein, Numerical Data and Functional Relationships in Science and Technology* (New Series, Group VI, Vol. 2b), Springer Verlag, Berlin.
van den Bergh, S. and Hagen, G.L.: 1975, *AJ* **80**, 11.
Vogt, N. and Moffat, A.F.J.: 1975, *A&A* **39**, 477.